Microelectronics Reliability 91 (2018) 31–37

Contents lists available at ScienceDirect

Microelectronics Reliability

journal homepage: www.elsevier.com/locate/microrel

Heavy ion impact on narrow band cascoded low noise amplifier

P. Rajendiran*, R. Srinivasan

Department of Information Technology, SSN College of Engineering, Kalavakkam 603 110, Tamil Nadu, India

ARTICLE INFO

Keywords:
Heavy ions
LNA
MOSFET
Single event effects
Single event transient
Source degeneration inductor

ABSTRACT

The impact of heavy ion strike on a cascoded narrow band low noise amplifier (LNA) is analyzed in this work using numerical device simulations. The impact is analyzed in the time as well as the frequency domains. The LNA uses 45 nm channel length MOSFETs. The most vulnerable portion of the most vulnerable device is chosen for irradiation study. As a part of the study, the influence of the source degeneration inductor of the LNA on single event impact is analyzed. The collected charge due to single event transient current reflects the severity of the radiation strike, and the same is taken as the performance metric in the study. It was found that the larger value of source degeneration inductor mitigates the SET impact but it trades off with the gain and noise figure of the LNA.

1. Introduction

Commercial and consumer RF based CMOS applications have evolved from 0.8 GHz to 10 GHz [1] (i.e. GPS, CDMA, WLAN, etc.) (mm-wave) which once was dominated by III-V compound semiconductor technology. The CMOS technology scaling improves the cut-off frequency (f_t), maximum oscillation frequency (f_{max}) and minimum noise figure (NF) [2–4] performance. Remarkable RF device characteristics have been reported for SiGe bipolar/BiCMOS [5–7], Si-bipolar/BiCMOS [8–10] and RF CMOS technologies [11,12]. RF CMOS blocks allow the integration of RF front-end and base-band circuitry on the same chip, without any additional investments [13].

While the CMOS scaling is enjoying benefits it challenges us from the process variations and reliability perspective. One of the important reliability issues is the performance of the CMOS in the radiation environment. Using the CMOS technology in the radiation prone environment, and the increased sensitivity of scaled CMOS devices demand to study the heavy ion or single event effects (SEE) performance of these systems. SEE damages may be temporary, known as soft errors or permanent, known as hard errors [14].

Soft errors in SRAM cells have been explored extensively and globally, the researchers are focused on the radiation effects in the digital integrated circuits [15–19]. Literatures have reported the impact of SET (single event transient - a form of SEE) in voltage controlled oscillators and phase locked loops (PLL) [20–23]. In RF integrated chips, the front end blocks especially the low noise amplifier (LNA) plays a key role in deciding the overall reception performance. A radiation-hardened, wideband LNA for satellites in the Van Allen radiation belts has been reported on a commercial 0.25 μm SiGe-BiCMOS process [24]. SEE performance of LNAs, mixers, and analog to digital converters is yet to be studied in detail. Heavy ion strike leads to SET, and SET results in further consequences. If it is a SRAM then SET may lead to single event upset (SEU). In LNA, SET results in output wave form distortion during the strike.

In this work, a cascoded LNA is studied for its SET performance using numerical device simulations. Since these distortions are ephemeral, the LNA output is investigated both in the time and the frequency domains in this work. In a typical receiver, a mixer follows the LNA, and the mixer is a frequency selective/conversion system. Therefore the frequency domain analysis of the LNA output during radiation helps us to design a mixer stage. 'Collected charge' is taken as a metric for the time domain investigation, and 'spectrogram' is used for frequency domain investigation. Section 2 provides the details of the device calibration, and Section 3 deals with the cascoded LNA topology used in this study along with the performance metrics of LNA. Section 4 describes SEE simulation on LNA and Time domain analysis. Section 5 provides the details of the frequency domain analysis of SET Simulation Results and Section 6 concludes the work.

2. Device calibration

In this section, the nMOSFET device used in the LNA circuit is simulated and calibrated against the published results [25]. DC device simulation facility of the Sentaurus TCAD simulator from is used for this purpose. The structural and doping information of the device are given in Table 1. In device simulation, the doping dependency mobility

---

* Corresponding author.
E-mail address: rajvastiram@gmail.com (P. Rajendiran).

https://doi.org/10.1016/j.microrel.2018.08.001
Received 20 April 2018; Accepted 1 August 2018
0026-2714/

Table 1
MOS device parameters.

Parameters	Values
Gate length (L)	45 nm
Gate oxide thickness (t_{ox})	2 nm
Gate work function (ϕ_m)	4.1 eV
Substrate doping	5e17 cm^{-3}
Source/drain doping (Ns and Nd)	1e20 cm^{-3}

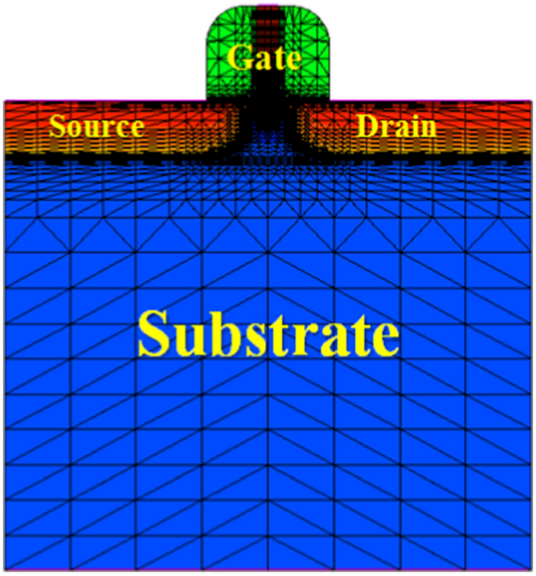

Fig. 1. Simulated nMOSFET device structure.

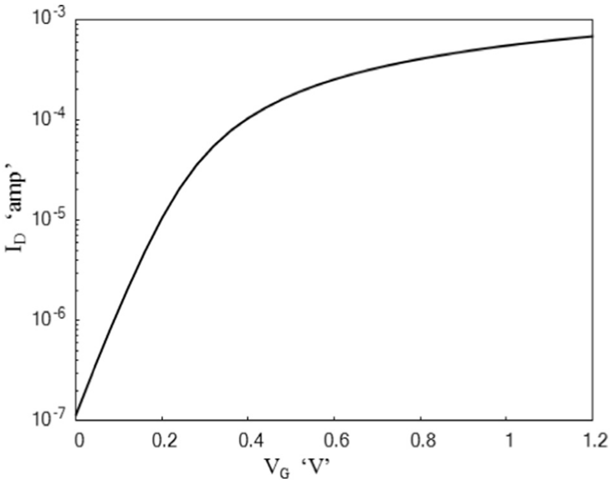

Fig. 2. $I_D - V_G$ characteristics of the device used in LNA circuit for this study.

models, recombination models, velocity saturation models and quantum correction models are invoked. The I_D-V_G characteristics of the calibrated device are shown in Figs. 1 and 2.

3. Cascoded LNA topology

The cascoded LNA circuit, common source (CS) followed by a common gate (CG) configuration, used in this work is discussed in this section. The LNA circuit is shown in Fig. 3, and in this circuit the required input impedance matching is attained mainly through the source-degenerative inductor (LS) [26,27] depicted in Fig. 3. The choice of LS controls the real part of input impedance, and the input impedance of LNA is matched to (50 + j0) Ω at 10 GHz, over a narrow band frequency [26,27].

We assume a quality factor of 5 for all the inductors (LS, LG, and LD) of the LNA circuit, and necessary resistors are connected in series with the corresponding inductors. The discussed LNA circuit is simulated using the mixed mode DC and AC simulation facilities available in the simulator. Apart from the models listed in the Section 2, noise models are included in the device simulations while doing the noise simulation of the LNA. The device and bias details of the LNA circuit is given in Table 2. The LNA performance metrics like the input impedance (Zin (real) and Zin(imaginary)), gain (S21), non-linearity (IIP3) and Noise Figure (NF) are provided in Table 2, @ 10 GHz. Fig. 4 depicts the Gain, Noise Figure and Input impedance (Zin) ohms (real and imaginary) as a function of frequency. We can see from Fig. 4 that the input impedance matching is achieved @ 10 GHz.

4. SEE simulation on LNA and time domain analysis

The heavy ion simulation set up and the heavy ion models are discussed in this section. Transient simulations are used to perform the heavy-ion strike on the LNA circuit discussed in Section 3. Apart from the models listed in Section 2, the heavy-ion models are included for SEE simulations. Heavy ions are characterized using the particle direction (perpendicular to the device), characteristic radius (10 nm in this study), length of the ion track (1.5 μm in this study), Linear Energy Transfer (LET in MeV/(mg/cm^2)), and the strike location. Fig. 5 depicts the SET simulation methodology of LNA circuit. The SET study is performed at six different locations,

- L1 - channel closer to source of M1
- L2 - channel center of M1
- L3 - channel closer to drain of M1
- L4 - channel closer to source of M2
- L5 – channel centre of M2
- L6 – channel closer to drain of M2

4.1. Time domain analysis of SET simulation results

vout(t) and i(t), depicted in Fig. 3, are studied to understand the SET performance of the LNA, and are plotted as a function of time in Figs. 6 and 7, for 'No-radiation' and 'radiation' (LET of 10 MeV/(mg/cm^2)) cases. The striking location, for Figs. 6 and 7, is chosen to be the channel centre of M2 i.e. L5, with a dose value of 10 MeV/(mg/cm^2). 'No radiation' plots of Figs. 6 and 7 depict smooth sinusoidal oscillations. But the 'radiation' plots shown in Figs. 6 and 7 clearly depict the disturbance. The pre-radiation period, time $<$ 1.5 ns, has smooth vout (t) and i(t) wave forms ('radiation' case in Figs. 6 and 7). The radiation strike disturbs vout(t) and i(t), from 1.5 ns to 2.2 ns approximately, and smooth oscillations are obtained for time $>$ 2.2 ns, as can be seen from Figs. 6 and 7. The heavy-ion charge density generated in M2 during the peak radiation is shown in Fig. 8. The LNA metrics, input impedance, gain and noise figure get disturbed due to radiation strike. Fig. 9 depicts LNA metrics as a function of radiation dose. The parameters in Fig. 9 are extracted during the peak disturbance. We can observe from Fig. 9 that the input impedance, both real and imaginary, deviates more and more from 50 + j0 Ω, as the dose increases, and therefore the gain is expected to go down.

Collected charge (Q_C) due to radiation strike is used as a metric to quantify the SET impact. The Q_c can be calculated from the i(t) wave form in the absence of AC signal. Figs. 10 and 11 illustrate vout(t) and i (t) in the absence of AC signal, for 'No-radiation' and 'radiation' cases. The striking location, is once again is chosen to be L5, with a dose value of 10 MeV/(mg/cm^2). The collected charge (Q_c) is calculated by integrating the transient current 'i(t)' between the appropriate time limits,